Malays. J. Anal. Sci. Volume 29 Number 5 (2025): 1350

MALAYSIAN JOURNAL OF ANALYTICAL SCIENCES

Journal homepage: https://mjas.analis.com.my/

Research Article

Tailoring nanocellulose properties from spent coffee grounds via controlled sulphuric acid hydrolysis

Sabiha Hanim Saleh,[1,2] Nur Risha Umaira Shaiful Bahri,[1] Norizan Ahmat,[3] Shariff Ibrahim,[1,2] and Noraini Hamzah[1,2*]

[1]School of Chemistry and Environment, Faculty of Applied Sciences, Universiti Teknologi MARA, 40450 Shah Alam, Selangor, Malaysia
[2]Industrial Waste Conversion Technology Research Group, Faculty of Applied Sciences, Universiti Teknologi MARA, 40450 Shah Alam, Selangor, Malaysia
[3]Centre of Foundation Studies, Universiti Teknologi MARA, Cawangan Selangor, Kampus Dengkil, 43800 Dengkil, Selangor, Malaysia

*Corresponding author: pnoraini@uitm.edu.my

Received: 19 September 2024; Revised: 22 August 2025; Accepted: 25 August 2025; Published: 16 October 2025

Abstract
Spent coffee grounds (SCG) are an abundant agricultural residue rich in cellulose, which can be converted into nanocellulose (NC), a renewable, biodegradable material with high crystallinity and strength. However, extracting NC requires careful control of process conditions to maximise yield while preserving structural integrity. In this study, the effect of sulphuric acid (H_2SO_4) concentration on NC production from SCG cellulose was systematically investigated. Cellulose was first obtained via alkaline treatment and delignification, followed by acid hydrolysis at four H_2SO_4 concentrations (45, 50, 55, and 60 wt%) under controlled temperature, reaction time, and fibre-to-acid ratio. The yield of NC increased from 66.69 ± 0.81% at 45 wt% to 78.58 ± 1.90% at 60 wt%, with the crystallinity index rising from 54% in cellulose to above 90% at 50–55 wt%. The optimal condition was identified at 55 wt% H_2SO_4, achieving 77.24 ± 2.03% yield and 93% crystallinity while maintaining the NC structure. Thermal analysis showed reduced stability in NC compared to cellulose due to sulphate group incorporation. These results demonstrate that precise control of acid concentration is essential for producing high-quality NC from SCG for sustainable material applications.

Keywords: cellulose, nanocellulose, spent coffee grounds, sulphuric acid

Introduction

Spent coffee grounds (SCG), the solid residue obtained after brewing coffee, are among the most abundant by-products of the global coffee industry. Millions of tonnes are generated annually worldwide, and due to their low commercial value, they are often discarded in landfills, causing environmental concerns [1,2]. Disposal in landfills contributes to leachate generation and greenhouse gas emissions, particularly methane, which accounts for approximately 20% of global anthropogenic methane output [3]. Given the scale of waste generation and its environmental footprint, sustainable valorisation of SCG is urgently needed. In response, researchers and industry have explored various methods to repurpose SCG to mitigate environmental impacts. Spent coffee grounds have been utilised as chemical feedstocks [4], for biodiesel production [5], in aerogel preparation [6], and for food science applications [7]. Notably, SCG are rich in cellulose, a major structural component of plant cell walls. This cellulose, found abundantly in SCG, can be extracted and utilised in various industrial applications. Specifically, cellulose derived from SCG can be processed into nanocellulose (NC), a material known for its high strength, low weight, and biodegradability.

By transforming SCG into NC, this agricultural waste can be converted into valuable products, thereby supporting sustainable waste management and reducing the environmental pollution associated with SCG disposal. Although sulphuric acid (H_2SO_4) is used in the process, proper recovery and neutralisation steps can mitigate its environmental impact. Spent

coffee grounds were selected due to their abundance, underutilisation, and high lignocellulosic content, making them a promising source for NC production. The feedstock used in this study exhibited compositional characteristics that differ from those reported in the literature, offering an opportunity to examine how these differences interact with H_2SO_4 concentration to influence the crystallinity and physicochemical properties of the resulting NC.

Cellulose is the most abundant natural polymer found in plant cell walls [8]. It is accompanied by other components of lignocellulosic materials, such as hemicellulose, lignin, and extractives [9]. Typically, cellulose extraction from plant cell walls begins with delignification to remove lignin, followed by alkali treatment to eliminate hemicellulose and other compounds [10]. The extracted cellulose can then be used to produce NC through acid hydrolysis. Nanocellulose, also referred to as cellulose nanomaterials, can be categorised into two groups: cellulose nano-objects and cellulose nanostructured materials. Cellulose nano-objects include cellulose nanocrystals and cellulose nanofibrils, while cellulose nanostructured materials consist of cellulose microcrystals and cellulose microfibrils [11]. Due to its nanoscale diameter, NC exhibits high strength, stiffness, and a large surface area, making it ideal for use in the production of nanomaterials [12]. Additionally, NC is often preferred over conventional cellulose in high-value applications due to its advantages, as the hygroscopic nature and lack of melting properties of cellulose can limit its use [13].

Several methods are employed for extracting NC, including enzymatic hydrolysis and acid hydrolysis. However, enzymatic hydrolysis requires a lengthy operation time and is therefore often combined with other techniques [12]. Consequently, acid hydrolysis, which is straightforward to apply, was used to produce NC in this study. During acid hydrolysis of cellulose, the amorphous regions are preferentially disrupted, while the crystalline regions remain intact [14]. In this study, the concentration of H_2SO_4 is the main parameter investigated during hydrolysis, as it can significantly affect NC yield and crystallinity. Changes in H_2SO_4 concentration were made to study the relationship between acid concentration and physicochemical characteristics, as well as to determine the optimal concentration for NC production from SCG. Moreover, the quality of nanocellulose depends on both the type of SCG and the hydrolysis process. In particular, varying the concentration of H_2SO_4 can influence the structure and properties of the resulting nanocellulose, an effect that is poorly understood. This study aims to address this knowledge gap.The characteristics of the NC produced from SCG were analysed using Fourier transform infrared (FTIR) spectroscopy, field emission scanning electron microscopy (FESEM), X-ray diffraction (XRD), and thermogravimetric analysis (TGA).

Materials and Methods

Materials

Spent coffee grounds were collected from He & She Cafe in UiTM Shah Alam, Selangor, Malaysia. The samples were washed and dried in an oven at 60 °C for 6 h, ground, and sieved to a particle size of 0.5 mm. The chemicals used were ethanol (95%), sodium hydroxide (NaOH, 98%), H_2SO_4 (95–98%), sodium chlorite ($NaClO_2$, 80%), and glacial acetic acid (99%), all purchased from Sigma-Aldrich. All chemicals were of reagent grade unless otherwise stated.

Chemical composition analysis of SCG

The analysis of extractives was conducted following the method described by [15]. A 10 g sample was mixed with 5% ethanol in 200 mL of distilled water. The mixture was placed in a water bath at 80 °C for 3 h, cooled to room temperature, and then filtered using Whatman filter paper (pore size of 100 μm). The filtered sample was dried at 105 °C until a constant dry weight was obtained. Hemicellulose content was determined according to the procedure described by [16]. A 1 g sample of the dried extractive was mixed with 10 mL of 0.5 M NaOH solution. The mixture was heated in a water bath at 80 °C for 3.5 h. After heating, the solution was then rinsed with distilled water and filtered until a neutral pH was achieved. The resulting solution was dried at 105 °C, and the hemicellulose content was determined by weighing. The method for determining lignin content was adapted from [17]. A 1 g extractive sample was mixed with 15 mL of 72% H_2SO_4, stirred thoroughly, and left at room temperature for 4 h. Afterwards, 560 mL of purified water was added to the mixture. The solution was heated to 100 °C for 4 h. The mixture was then cooled to room temperature and filtered. The lignin was dried overnight, cooled for 1 h, and then weighed. The cellulose content was estimated by subtracting the sum of hemicellulose, lignin, and extractives from 100.

Alkali treatment

Alkali treatment was carried out using a 4% w/v NaOH solution at 120 °C for 3 h, with continuous stirring and a sample-to-solution ratio of 1:20 g/mL. After treatment, the sample was filtered and rinsed several times with distilled water to remove any residual alkali solution [10].

Delignification

The delignification process, adapted from [16], was employed to remove lignin, pectin, and extractives. The alkali-treated sample was immersed in hot

distilled water at 75 °C for 1 h using a 1:20 g/mL ratio of sample to hot distilled water. Following this, the fibre was treated with a 0.7% w/v acidified $NaClO_2$ solution at 75 °C for 2 h, with continuous stirring at 400 rpm. The pH of the $NaClO_2$ solution was adjusted to 4 using 4% v/v glacial acetic acid. The ratio of fibre to acidified $NaClO_2$ solution was 1:25 g/mL. The acidified $NaClO_2$ delignification step was repeated several times until the fibre turned white. The residue was then vacuum filtered, washed multiple times with distilled water until the pH was neutral, and oven-dried overnight at 50 °C before proceeding to the next step.

Acid hydrolysis

The delignified SCG were hydrolysed using a H_2SO_4 solution at a fibre-to-acid ratio of 1:20 g/mL. Four concentrations of H_2SO_4 (45, 50, 55, and 60 wt%) were used to investigate the effect of acid concentration on the properties of the resulting NC. For each concentration, the mixture was heated at 45 °C for 30 min and then diluted in an ice bath to stop the reaction. The fibres were centrifuged twice at 2,500 rpm for 10 min using deionised water to reduce the acid concentration. Washing and dialysis were repeated until the pH reached neutrality. The suspensions were subjected to probe sonication (200 mL, 40 kHz, 60 W) at 25 °C for 10 min, as described by [18]. After acid hydrolysis, the yield of NC was determined according to Equation 1.

$$\text{Yield (\%)} = W_f/W_i \times 100\% \quad (1)$$

Where W_f is the dry weight of the NC obtained (g) and W_i is the dry weight of the initial material used for hydrolysis (g).

Characterisation

Fourier transform infrared analysis

An FTIR spectrometer (Spectrum One, PerkinElmer, US) was used to obtain the spectra of the SCG, cellulose, and NC samples. The wavenumber for each sample was set in the range of 650–4000 cm^{-1} with a resolution of 4 cm^{-1} and a total of 16 scans.

Field emission scanning electron microscopy

The microstructure of the sample surface was analysed using FESEM (JEOL JSM 6460, Japan). The sample was first coated to gain high-resolution images. An accelerating voltage of 2 kV and 2,500× magnification was used during the examination of the samples.

X-ray diffraction

X-ray diffraction analysis was performed using a diffractometer (PANalytical X'Pert Pro, Netherlands) fitted with a copper target (λ = 0.154 nm) at an acceleration voltage of 40 kV and a current of 15 mA. Diffraction measurements were recorded over a 2θ range of 5°–90° at a scanning speed of 3°/min. The crystallinity index (CI) was calculated from the diffraction patterns (Equation 2), while the crystallite size (L) was estimated using the Scherrer equation, as described by [19] (Equation 3).

$$CI\ (\%) = \frac{A_{crys}}{A_{total}} \times 100\% \quad (2)$$

Where A_{crys} is the area of crystalline peaks and A_{total} is the total area of all peaks.

$$L = k\lambda/B\cos\theta \quad (3)$$

Where k is the shape factor (typically taken as 0.94), λ is the wavelength of the XRD radiation (0.154 nm), and B is the full width at half maximum of the diffraction peaks.

Thermogravimetric analysis

Thermogravimetric analysis was carried out according to the method outlined by previous study [20]. Approximately 10 mg of each sample was placed in the instrument (TA Instruments Q500, US), and the analysis was conducted with a nitrogen flow rate of 100 mL/min and a heating rate of 10°C/min, covering a temperature range from 40 to 850 °C. The data were then recorded.

Results and Discussion

Chemical composition of SCG

The chemical composition of the SCG is presented in **Table 1**. The analysis indicates 2.7 ± 0.4% ethanol extractives, although no direct comparison is available in the literature, specifically for SCG. Hemicellulose content was 29.41 ± 3.3%, which falls within the typical range reported for SCG (25–39.1%) [21,22], indicating moderate levels. Lignin was measured at 24.2 ± 3.0%, slightly higher than some reported values (12–23.9%) [21,22], but still within the broader literature range, suggesting a moderate amount. The cellulose content was 43.69%, higher than the 30.2% reported by [21] and the 12.4% reported by [22], placing it towards the upper end of reported ranges.

Overall, the SCG sample exhibits substantial cellulose and hemicellulose, moderate lignin, and minimal ethanol extractives, reflecting a composition typical of SCG. Although SCG composition can vary depending on factors such as brewing method, growing conditions, and coffee type, most SCG share a similar general profile. The largest component of SCG is polysaccharides, specifically cellulose and hemicellulose, which together constitute around 50% of the dry mass.

Table 1. Chemical composition of SCG

Content	% Composition
Ethanol extractives	2.70 ± 0.4
Hemicellulose	29.41 ± 3.3
Lignin	24.20 ± 3.0
Cellulose	43.69 ± 2.2

Yield of nanocellulose

This study focused on varying H_2SO_4 concentration, as it is one of the most influential parameters in acid hydrolysis, directly affecting the removal of amorphous regions, crystallinity, particle size, and surface charge of NC. Other factors, including temperature, reaction time, and fibre-to-acid ratio, were kept constant based on optimised conditions reported in previous studies to minimise variability and isolate the effect of acid concentration. This approach enabled a systematic evaluation of the influence of acid concentration alone on NC yield and physicochemical properties, while ensuring comparability with the literature. The obtained cellulose from the delignification process was subjected to acid hydrolysis to extract NC. Figure 1 shows the NC obtained by employing various concentrations of H_2SO_4 (45, 50, 55, and 60 wt%).

The yield of NC increased with higher H_2SO_4 concentrations, as shown in **Table 2**. At 45 wt% H_2SO_4, the yield was 66.69 ± 0.81%, which increased to 70.64 ± 3.02% at 50 wt%. Further increases to 55 wt% and 60 wt% resulted in yields of 77.24 ± 2.03% and 78.58 ± 1.90%, respectively. This trend is attributed to the chemical action of H_2SO_4, which selectively hydrolyses the amorphous regions of cellulose while leaving the crystalline regions largely intact. At lower acid concentrations, hydrolysis is partial, resulting in lower yields. As the concentration increases, more amorphous cellulose is broken down, leading to higher NC yields. Beyond 60 wt%, the yield plateaus because most amorphous regions have already been removed, and excessive acid may start to degrade the crystalline regions, limiting further improvements [23,25].

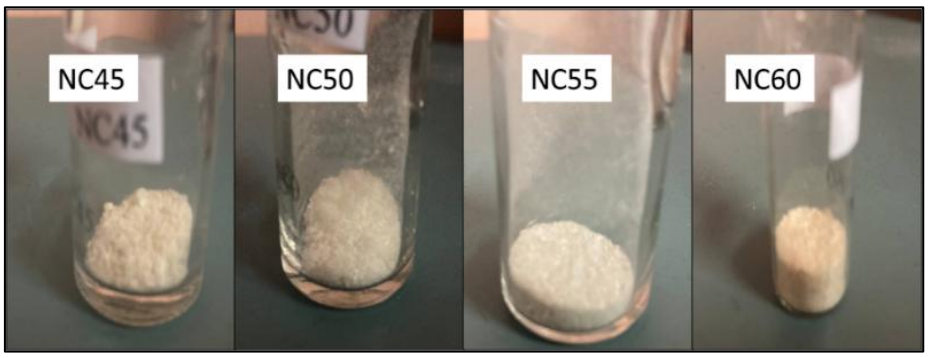

Figure 1. Nanocellulose obtained after acid hydrolysis

Table 2. Yield of NC prepared from different concentrations of H_2SO_4

H_2SO_4 Concentration (wt%)	Yield of NC (%)
45	66.69 ± 0.81
50	70.64 ± 3.02
55	77.24 ± 2.03
60	78.58 ± 1.90

FTIR analysis

The FTIR spectra of the raw samples, cellulose, and NC samples are displayed in **Figure 2**. These spectra demonstrate spectroscopic evidence of structural changes in the untreated sample, as well as during different stages of treatment. These stages include after delignification and acid hydrolysis. The cellulose yield was obtained by employing $NaClO_2$ in the delignification process. During this step, $NaClO_2$ oxidises and cleaves the aromatic rings and ether linkages of lignin, converting them into soluble compounds and thereby facilitating the isolation of cellulose. The completion of the removal of hemicellulose was indicated by the disappearance of peak values of 2925 and 2582 cm^{-1}, which were attributed to the asymmetrical and symmetrical stretching of CH_2 in hemicellulose. This indicates that NaOH treatment saponified ester bonds and removed hemicellulose, leaving a cellulose-rich fraction. The cellulose spectrum shows the properties of pure cellulose as the O-H and C-O stretching vibrations can be found at 3400 and 1060 cm^{-1}, respectively, with the addition of the glycosidic C1 deformation that can be observed at 897 cm^{-1} [26].

After the acid hydrolysis treatment, the peak ranges from 1230 to 1220 cm^{-1}, which was absent in the raw and cellulose samples, appeared in all NC spectra. This is attributed to the mechanism during acid hydrolysis using H_2SO_4, where the SO_4^{2-} attacks the C6 position of the cellulose pyranose ring, as there is less steric hindrance at C6 compared to other carbon ring sites [18]. This selective hydrolysis removes amorphous domains of cellulose while leaving crystalline regions intact, leading to the formation of NC. At the range of 1160–1150 cm^{-1} (C-O-C pyranose ring), the intensity of the band decreased after H_2SO_4 treatment. The hydrolysis occurring at the skeletal C-O-C pyranose ring caused disruption of the cellulose ring [18]. The bands range from 1030 to 1020 cm^{-1} correspond to cellulose C-O stretching vibrations, which are present in all spectra [27]. The band at 3400 and 1427 cm^{-1} in all spectra indicates that delignification and hydrolysis did not alter the chemical structure of the SCG. The FTIR findings provide a chemical basis for both the structural integrity and functional performance of the NC, guiding its potential application in suspension-based materials and biocomposites.

FESEM analysis

Field emission scanning electron microscopy was used to observe the surface morphological characteristics of the extracted NC. After being treated with varying concentrations of H_2SO_4, the surface morphology of the fibres was found to undergo noticeable transformations. There is a distinct morphological difference between cellulose and the samples of NC, which can be identified as shown in Figure 3. The cellulose fibre exhibited a smoother and more uniform surface than the NC samples (**Figure 3(a)**). Following acid hydrolysis, the surface of the fibre was altered, and it became more abrasive, showing holes and cracks with an irregular multilayer surface, which can be observed in **Figure 3(b–e)**. This change is a result of a process known as fibrillation, which involves the elimination of amorphous components such as hemicellulose, lignin, and extractives [20]. During this stage, H_2SO_4 preferentially hydrolyses the glycosidic bonds in the amorphous regions of cellulose, leading to fragmentation of the fibres into smaller fibrils and exposing the crystalline domains.

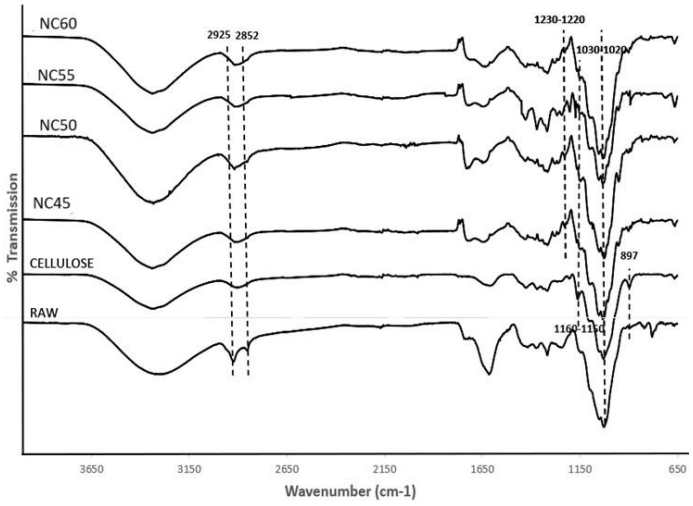

Figure 2. FTIR spectra of SCG (raw), cellulose, and NC samples

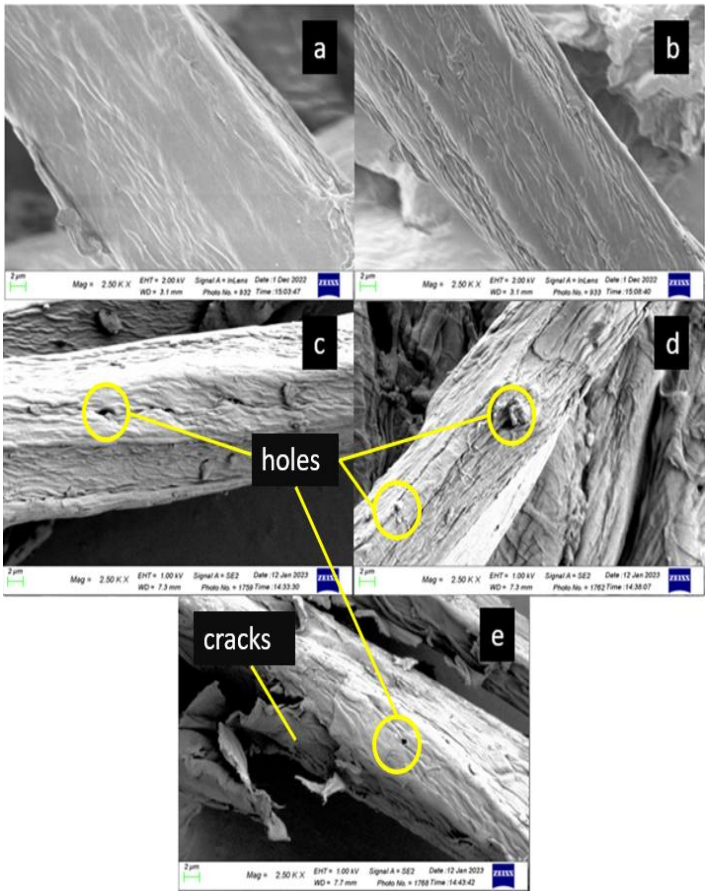

Figure 3. FESEM morphology of a) cellulose and individual NC fibres prepared from different concentrations of H_2SO_4: b) NC45, c) NC50, d) NC55, and e) NC60

Sulphuric acid plays a role in the efficient defibrillation of the amorphous content. However, as the concentration increases, the surface becomes more damaged. This is because higher acid concentrations not only hydrolyse the amorphous regions but also begin to erode crystalline cellulose, causing excessive degradation and surface collapse. The surface of the NC treated with a low concentration of H_2SO_4 experienced the least amount of damage when compared to the surface of the NC treated with 60 wt% acid concentration. Although it is necessary to achieve optimal elimination of the amorphous region, it is preferable to use an ideal concentration for the fibrillation process that does not completely damage the properties of the NC [28]. In addition, the extraction of NC produced a rod-like structure, which is commonly observed during acid hydrolysis [27]. The FESEM results highlight the structural differences between cellulose and NC and emphasise the need to optimise acid concentration for effective fibrillation without damaging the structure.

XRD analysis

Figure 4 presents the XRD patterns and CI of cellulose and NC derived from SCG. Achieving a high degree of crystallinity is essential for enhancing the performance of NC, as it affects both its thermal and mechanical resistance [20]. During alkali treatment, NaOH removes hemicellulose and saponifies ester linkages, improving cellulose purity. This is followed by delignification using $NaClO_2$ under acidic conditions, where lignin aromatic structures are oxidatively cleaved, further exposing the cellulose microfibrils. Finally, H_2SO_4 hydrolysis preferentially attacks the amorphous regions of cellulose through protonation of glycosidic oxygen, leading to cleavage of β-1,4-glycosidic bonds. This selective hydrolysis eliminates disordered domains while preserving crystalline regions, thereby increasing CI. As expected, CI increased with higher concentrations of H_2SO_4 because hydronium ions penetrate the amorphous regions of cellulose, cleaving glycosidic bonds and releasing crystallites [10]. However, the acid hydrolysis treatment using 60 wt% caused a slight reduction in the CI. A similar finding was

reported by previous study [27], where concentrations of 35, 45, and 55 wt% yielded high CI values, but CI decreased when 65 wt% of H_2SO_4 was employed. At excessively high concentrations, the harsh conditions hydrolyse not only the amorphous regions but also parts of the crystalline domains, thereby lowering CI [29].

The crystallite sizes of the NC samples were determined using the Scherrer equation. Crystallite size, defined as the average dimension of crystals perpendicular to the hkl plane, provides insights into the thermal stability of the sample [20]. The crystallite sizes for NC45, NC50, NC55, and NC60 were 15.82, 10.38, 9.03, and 8.65 nm, respectively, as shown in **Table 3**. Mamat Razali et al. [30] found that smaller crystallite sizes can enhance the nanomechanical properties of cellulose by enabling better structural symmetry. A high CI combined with a small crystallite size indicates effective removal of amorphous regions [31]. Therefore, smaller crystallite sizes are generally preferred for improved NC formation. Although the 60 wt% H_2SO_4 treatment yielded the smallest crystallite size, the accompanying reduction in CI at this concentration makes the 55 wt% H_2SO_4 treatment more favourable. Furthermore, XRD analysis confirms the increased crystallinity of NC, supporting its enhanced mechanical properties and potential as a reinforcing agent in biocomposites.

Thermal behaviour

There are three distinct regions of mass loss visible across all the samples, as illustrated in **Figure 5**. The first stage, occurring below 230 °C, involves a slight mass decrease (<10%). The mass loss at this stage is due to the evaporation of moisture and the combustion of volatile chemicals present in the samples [16]. The major mass loss occurs between 230 and 350 °C. At this stage, cellulose undergoes pyrolysis, involving the decomposition and depolymerisation of glycosyl units [32]. When all the samples were heated to 550 °C, NC45, NC50, NC55, and NC60 lost 76%, 74%, 60%, 54%, and 53% of their mass, respectively. These results indicate that NC treated with higher concentrations of H_2SO_4 exhibits lower mass loss, due to the presence of sulphate groups in the cellulose chains that act as a flame retardant [20].

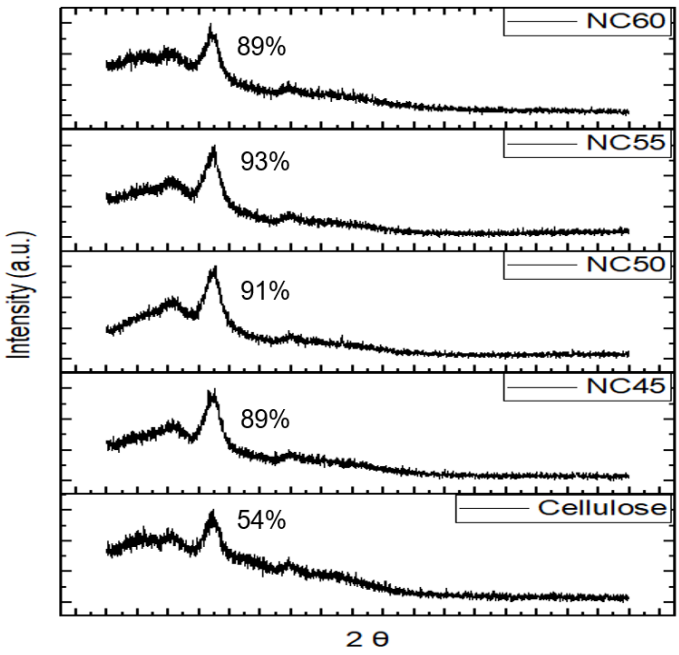

Figure 4. XRD pattern of cellulose and NC after treatment with different concentrations of H_2SO_4

Table 3. Crystallite sizes for NC samples

NC	Crystallite Size (nm)
NC45	15.82
NC50	10.38
NC55	9.03
NC60	8.65

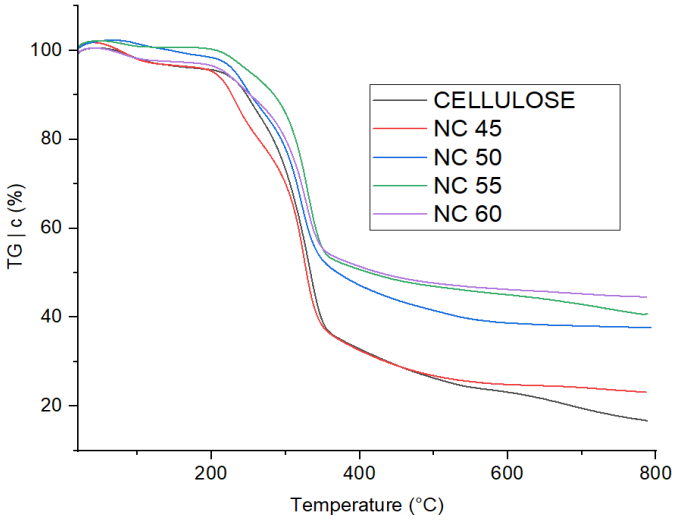

Figure 5. TGA curves of cellulose and NC prepared with various H_2SO_4 concentrations

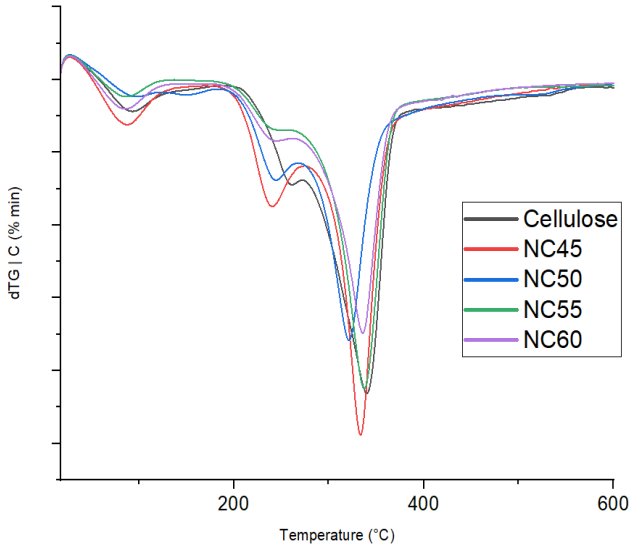

Figure 6. DTGA curves of cellulose and NC prepared with various H_2SO_4 concentrations

Figure 6 displays the derivative thermogravimetric analysis (DTGA) curves for the samples. The maximum degradation temperatures were 340 °C for cellulose, 333 °C for NC45, 321 °C for NC50, 337 °C for NC55, and 335 °C for NC60. In comparison with cellulose, the NC samples exhibited lower thermal stability as a result of acid hydrolysis. This decrease in thermal stability is due to the presence of sulphate groups in the NC, as these groups decompose at lower temperatures [16]. Maciel et al. [20] also noted that H_2SO_4 hydrolysis substitutes -OH groups with sulphate groups, further reducing the thermal stability of cellulose crystals. This effect is associated with the lower activation energy required for the degradation of NC, resulting in reduced thermal resistance under inert conditions. The TGA results highlight the decreased thermal stability of NC, a factor that must be considered when selecting processing conditions for heat-sensitive applications.

Conclusion

This study successfully extracted NC from SCG using H_2SO_4 hydrolysis, achieving a high yield of 77.24 ± 2.03% at the optimal concentration of 55 wt% H_2SO_4. A significant increase in crystallinity was confirmed in XRD analysis, from 54% in cellulose to 93% in NC, while FTIR analysis verified the removal of lignin and hemicellulose. Furthermore, FESEM revealed the transformation of cellulose fibres into rod-like nanostructures, and TGA indicated reduced thermal stability due to the introduction of sulphate groups. Overall, the combination of high yield, enhanced crystallinity, and well-preserved morphology highlights the strong potential of NC as a reinforcing

agent in biocomposites and suspension-based materials.

Acknowledgement
The authors are grateful to the Ministry of Higher Education, Malaysia for the financial support provided for this research through grant number FRGS/1/2022/STG 04/UITM/02/10.

References

1. An, B. H., Jeong, H., Kim, J.-H., Park, S., Jeong, J.-H., Kim, M. J. and Chang, M. (2019). Estrogen receptor-mediated transcriptional activities of spent coffee grounds and spent coffee grounds compost, and their phenolic acid constituents. *Journal of Agricultural and Food Chemistry,* 67 (31): 8649-8659.
2. McNutt, J. and He, Q. (2019). Spent coffee grounds: A review on current utilization. *Journal of Industrial and Engineering Chemistry,* 71: 78-88.
3. Sallam, R. M. A. (2020). Landfill emissions and their impact on the environment. *International Journal of Chemical Studies*, 8 (2): 1567-1574.
4. Vardon, D.R., Moser, B.R., Zheng, W., Witkin, K., Evangelista, R.L., Strathmann, T.J., Rajagopalan, K. and Sharma, B.K. (2013). Complete utilization of spent coffee grounds to produce biodiesel, bio-oil, and biochar. *ACS Sustainable Chemistry & Engineering,* 1: 1286–1294.
5. Shi, C., Chen, Y., Yu, Z., Li, S., Chan, H., Sun, S., Chen, G., He, M. and Tian, J, (2021). Sustainable and superhydrophobic spent coffee ground-derived holocellulose nanofibers foam for continuous oil/water separation. *Sustainable Materials and Technologies*, 28: e00277
6. Luo, X., Zhou, L., Wang, Y., Xiang, J., Zhang, H., Tao, R., Li, J., Wang, B. and Chen, R. (2024). Spent coffee ground-based cellulose nanofiber/reduced graphene oxide aerogel for efficient solar-driven interfacial evaporation via directional freezing technology. *Industrial Crops & Products,* 214: 118528.
7. Choe, U. (2025). Valorization of spent coffee grounds and their applications in food science. *Current Research in Food Science,* 10: 101010.
8. Gupta, P. K., Raghunath, S. S., Prasanna, D. V., Venkat, P., Shree, V., Chithananthan, C., Choudhary, S., Surender, K. and Geetha, K. (2019). An update on overview of cellulose, its structure and applications. In Cellulose. IntechOpen, UK: pp. 1-21.
9. Megashah, L. N., Ariffin, H., Zakaria, M. R. and Hassan, M. A. (2018). Properties of cellulose extract from different types of oil palm biomass. *IOP Conference Series: Materials Science and Engineering,* 368 (1): 012049.
10. Collazo-Bigliardi, S., Ortega-Toro, R. and Chiralt Boix, A. (2018). Isolation and characterisation of microcrystalline cellulose and cellulose nanocrystals from coffee husk and comparative study with rice husk. *Carbohydrate Polymers*, 191: 205-215.
11. Shen, R., Xue, S., Xu, Y., Liu, Q., Feng, Z., Ren, H., Zhai, H. and Kong, F. (2020). Research progress and development demand of nanocellulose reinforced polymer composites. *Polymers,* 12(9): 2113.
12. Phanthong, P., Reubroycharoen, P., Hao, X., Xu, G., Abudula, A. and Guan, G. (2018). Nanocellulose: Extraction and application. *Carbon Resources Conversion*, 1 (1): 32–43.
13. Trache, D., Tarchoun, A. F., Derradji, M., Hamidon, T. S., Masruchin, N., Brosse, N. and Hussin, M. H. (2020). Nanocellulose: From fundamentals to advanced applications. *Frontiers in Chemistry*, 6(8):392.
14. Aspler, J., Bouchard, J., Hamad, W., Berry, R., Beck, S., Drolet, F. and Zou, X. (2013). Review of nanocellulosic products and their applications. *Biopolymer Nanocomposites*, 461-508.
15. Vijayanand, C., Kamaraj, S., Karthikeyan, S. and Sriramajayam, S. (2016). Characterization of indigenous biomass. *International Journal of Agriculture Sciences,* 8(50): 2124-2127.
16. Bacha, E. G., Demsash, H. D. (2021). Extraction and characterisation of nanocellulose from eragrostis teff straw. *Research square,* 1-26.
17. Wang, Q. and Sarkar, J. (2018). Pyrolysis behaviors of waste coconut shell and husk biomasses. *International Journal of Energy Production and Management,* 3(1): 34-43.
18. Rashid, E. S. A., Gul, A., Yehya, W. A. H. and Julkapli, N. M. (2021). Physico-chemical characteristics of nanocellulose at the variation of catalytic hydrolysis process. *Heliyon,* 7(1): e07267.
19. Zergane, H., Abdi, S., Xu, H., Hemming, J., Wang, X., Willför, S. and Habibi, Y. (2020). Ampelodesmos mauritanicus a new sustainable source for nanocellulose substrates. *Industrial Crops and Products,* 144: 112044.
20. Maciel, M. M. Á. D., de Carvalho Benini, K. C. C., Voorwald, H. J. C. and Cioffi, M. O. H. (2019). Obtainment and characterisation of nanocellulose from an unwoven industrial textile cotton waste: Effect of acid hydrolysis conditions. *International journal of biological macromolecules,* 126: 496-506.
21. Zuluaga, R., Hoyos, C. G., Velásquez-Cock, J., Vélez-Acosta, L., Palacio Valencia, I., Rodríguez Torres, J. A. and Gañán Rojo, P. (2024). Exploring spent coffee grounds: Comprehensive morphological analysis and chemical

characterization for potential uses. *Molecules,* 29 (24): 5866.
22. Singh, T. A., N. Pal · P. Sharma, and Passari, A. K. (2023). Spent coffee ground: Transformation from environmental burden into valuable bioactive metabolites. *Reviews in Environmental Science and Biotechnology,* 22: 887-898.
23. Dhali, K., Ghasemlou, M., Daver, F., Cass, P. and Adhikari, B. (2021). A review of nanocellulose as a new material towards environmental sustainability. *Science of the Total Environment,* 775: 145871.
24. Tesfaye, A., Workie, F. and Kumar, V. S. (2022). Production and characterization of coffee husk fuel briquettes as an alternative energy source. *Advances in Materials Science and Engineering*, 2022: 1-13.
25. Tolessa, B. and Tibba, G. S. (2022). *Utilization of Coffee Husk as an Alternative Source: A Current Trend*. 42(1): 18-30.
26. Jiang, F. and Hsieh, Y. Lo. (2015). Cellulose nanocrystal isolation from tomato peels and assembled nanofibers. *Carbohydrate Polymers,* 122: 60-68.
27. Somphol, W., Prapainainar, P., Sae-Oui, P., Loykulnant, S. and Dittanet, P. (2018). Extraction of nanocellulose from dried rubber tree leaves by acid hydrolysis. *Materials Science Forum,* 936: 37-41.
28. Gonçalves, B. M. M., Camillo, M. de O., Oliveira, M. P., Carreira, L. G., Moulin, J. C., Neto, H. F., de Oliveira, B. F., Pereira, A. C. and Monteiro, S. N. (2021). Surface treatments of coffee husk fiber waste for effective incorporation into polymer biocomposites. *Polymers,* 13 (3428): 1-22.
29. Kusmono, Listyanda, R. F., Wildan, M. W. and Ilman, M. N. (2020). Preparation and characterization of cellulose nanocrystal extracted from ramie fibers by acid hydrolysis. Heliyon, 6(11): e05486.
30. Mamat Razali, N. A., Ismail, M. F. and Abdul Aziz, F. (2021). Characterization of nanocellulose from Indica rice straw as reinforcing agent in epoxy-based nanocomposites. *Polymer Engineering and Science*, 61(5): 1594-1606.
31. Dominic, M., Joseph, R., Begum, P. S., Kanoth, B. P., Chandra, J. and Thomas, S. (2020). Green tire technology: Effect of rice husk derived nanocellulose (RHNC) in replacing carbon black (CB) in natural rubber (NR) compounding. *Carbohydrate polymers*, 230(41): 115620.
32. Rashid, S. and Dutta, H. (2020). Characterisation of nanocellulose extracted from short, medium, and long grain rice husks. *Industrial Crops and Products,* 154: 112627.